ESKİŞEHİR TECHNICAL UNIVERSITY JOURNAL OF SCIENCE AND TECHNOLOGY A- APPLIED SCIENCES AND ENGINEERING

2019, 20(4), pp. 436 - 445, DOI: 10.18038/estubtda.513854

A FIRST-PRINCIPLES INVESTIGATION OF LITHIUM ADSORPTION AND DIFFUSION ON BN, AlN AND GaN MONOLAYERS

Sevil SARIKURT*

[1] Department of Physics, Faculty of Science, Dokuz Eylül University, 35390, İzmir, Turkey

ABSTRACT

We investigated the adsorption and diffusion of lithium atom on graphene like h-BN, h-AlN and h-GaN monolayers for potential applications as an anode for lithium ion batteries using first principles calculations. To find an energetically favorable site, three possible adsorption sites are considered to place the single Li atom on substrates. Our results revealed that lithium atom prefers the hollow site of the monolayer structures rather than the top of B, Al, Ga or N atom. We also obtained the diffusion energy barrier of adsorbed lithium ion through a pathway from one hollow position to another as 0.117, 0.452, and 0.610 eV for h-BN, h-AlN and h-GaN structures, respectively.

Keywords: III-V monolayers, Li-ion batteries, Adsorption energy, Diffusion energy barrier

1. INTRODUCTION

In recent years, tremendous attention has been paid to rechargeable Li-ion batteries (LIBs) due to their spectacular performance in comparison with other types of rechargeable batteries [1-5]. LIBs have a very wide application area such as hybrid electric vehicles, computer electronics, portable electronic devices [6-8]. Recently, several studies have been stated that two-dimensional (2D) materials such as graphene, phosphorene, borophene, silicene, antimonene can be promising potential candidates as anode materials for LIBs due to their superior electronic and mechanical properties [9-15]. Hexagonal boron nitride (h-BN), aluminum nitride (h-AlN) and gallium nitride (h-GaN) have also received great attention, because of having wide energy band gap, high thermal conductivity and high stability [16-19]. Previously, Zeng et al. [20] pointed out that h-BN nanosheets have better thermal and chemical stability comparing to graphene. Hence, these graphene-like materials can be proposed as a prominent nanoscale material.

There are various studies about h-BN, h-AlN and h-GaN nanostructures with adsorbed transition metal atoms [21-25]. Hwang et al. [26] obtained the Li atom adsorption behaviour on h-BN monolayer using semi-empirical Grimme DFT-D2 method (dispersion corrected density functional theory (DFT) calculation method) and compared their results with the ones calculated by conventional DFT method. They reported that the Li atom is strongly physically adsorbed on the BN-nanosheet with dispersion-corrected DFT calculation and the H-site is the most favorable adsorption site. Most recently, Sengupta [27] performed calculations for binding energies, diffusion barriers for different reaction pathways and also for different concentrations of Li and Na adsorption on monolayer AlN using DFT with Grimme's DFT-D2 van der Waals correction term. The hollow site is found as the most favorable site for Li/Na and adsorption energies are obtained as 1.83 eV and 1.21 eV for single Li and Na atom, respectively. The diffusion barrier of Li is determined as 0.40 eV, whereas this value is 0.15 eV for Na.

*Corresponding Author: sevil.sarikurt@deu.edu.tr
Received: 17.01.2019 Published: 30.12.2019

In this paper, we investigated the adsorption of Li over h-XN (X=B, Al and Ga) monolayers via first-principles calculations. To gain further insight into the adsorption properties, we considered three different adsorption sites and determined the possible adsorption sites for each structure.

2. COMPUTATIONAL METHOD

Structure optimization, energy calculations, electronic band structures and density of states (DOS) analyses were performed in Quantum Espresso (QE) software package [28], based on DFT. For exchange-correlation functionals, generalized gradient approximation (GGA) [29] with Perdew-Burke-Ernzerhof (PBE) type functional was considered. To describe the interaction between the ions and electrons, Kresse-Joubert projector augmented wave (PAW) potential [30] was taken into account. The effect of van der Waals interaction was implemented using Grimme's DFT-D2 dispersion correction method [31]. For all calculations, the kinetic energy cutoff of the wave functions was set as 65 Ry, a 9x9x1 Monkhorst-Pack [32] k-mesh was employed to sample the first Brillouin zone and a 60-kpoints grid was used for plotting the electronic energy band. The structure optimization calculations were carried out using Broyden-Fletcher-Goldfarb-Shanno (BFGS) algorithm [33] until Hellmann-Feynman forces on each atom were less than 10^{-3} Ry/Bohr. Gaussian smearing method was chosen with a broadening width of 0.02 eV. The threshold for energy convergence was set to 10^{-6} Ry with a Davidson diagonalization algorithm [34]. In order to prevent the interactions between layers, a vacuum space of 20 Å was applied along the z-direction. To analyze the Li diffusion on h-BN, h-AlN and h-GaN monolayers, we performed the Climbing-Image Nudged Elastic Band (CI-NEB) [35] calculations implemented in QE. For the determination of minimum energy path (MEPs) of each elementary step, we used seven images including initial and final configurations.

3. RESULTS and DISCUSSIONS

For the sake of comparison, we firstly obtained structure optimization calculations for the bare h-XN monolayers. The optimized lattice parameters as 2.51, 3.11, 3.21 Å for h-BN, h-AlN and h-GaN, respectively and corresponding bond lengths are d_{BN}=1.45, d_{AlN}=1.80 and d_{GaN}=1.85 Å, which are compatible with the literature [27, 36-40]. The top view of the crystal structure of h-XN monolayers is illustrated in Figure 1 (a). In order to investigate Li adsorption and diffusion on substrates, unit cell of each monolayer has been enlarged to a (4x4x1) supercell. The lattice constants of these supercells are at least four times of Li_2 bond length (2.67 Å) [41, 42], hence Li adatom mimics to isolated atom on the substrates.

Present PBE calculations show that each considered monolayer has semiconductor characteristic with a wide band gap. Obtained band structures and corresponding projected density of states (PDOS) are given in Figure 1 (b-d). Single layer h-BN has a band gap of 4.64 eV, while h-AlN and h-GaN has 2.89 and 2.10 eV, respectively. According to Löwdin analysis, 0.40 electrons (e^-) transferred from boron to nitrogen atoms, this charge transfer is 1.09 e^- from Al to N and 0.92 e^- from Ga to N atom as expected according to ionization potentials of constituent atoms. These results of charge analysis are consistent with the previous studies in the literature [43, 44].

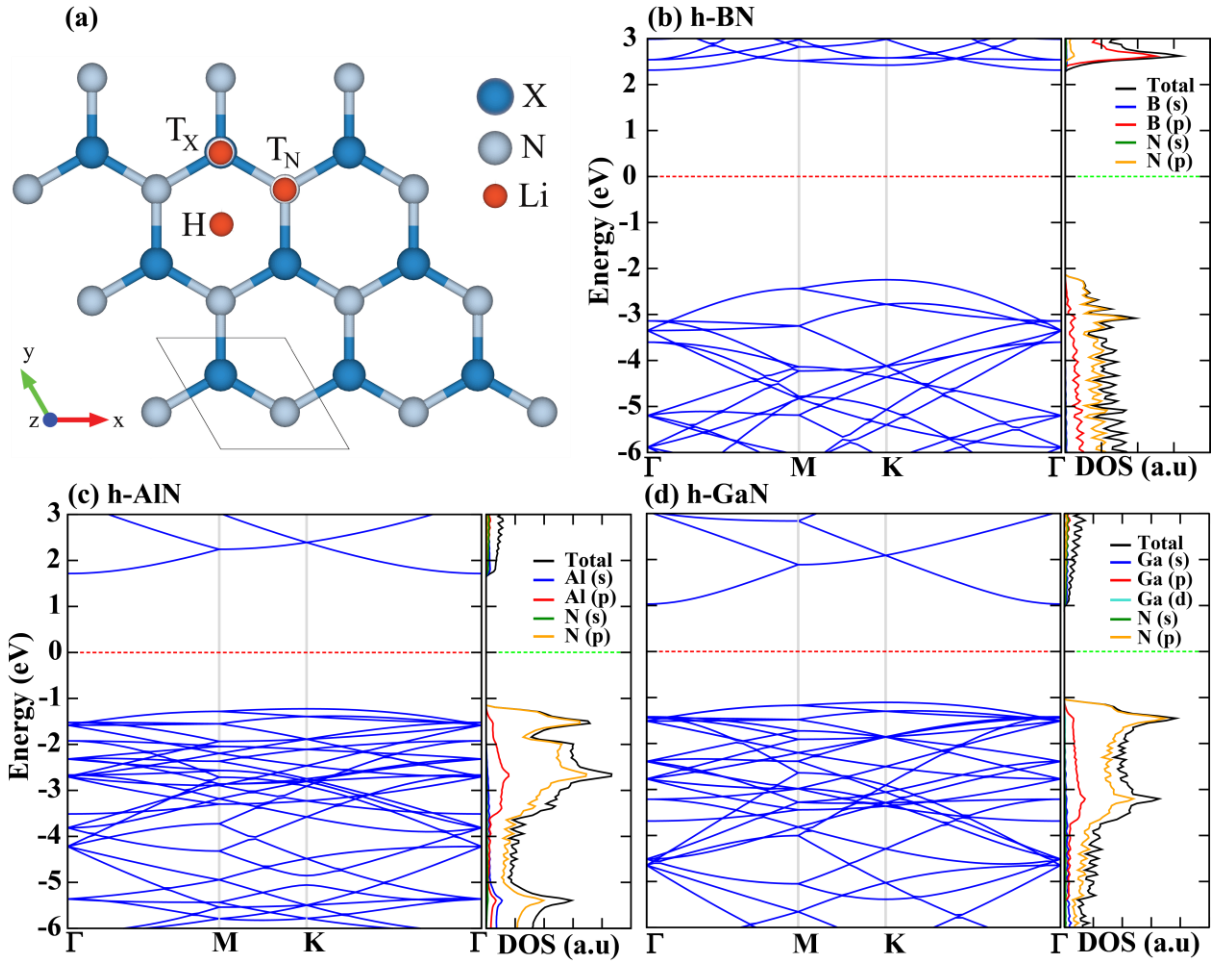


Figure 1. (a) Crystal structure of h-XN (X=B, Al, Ga) monolayer with three possible adsorptions sites of a single Li atom. (b-d) Electronic energy band structure, total and projected density of states (PDOS) for bare 4x4x1 supercell structures of h-BN, h-AlN and h-GaN.

To explore the Li adsorption behavior on h-BN, h-AlN and h-GaN, we considered three adsorption sites: (i) on the top of an X (X=B, Al, Ga) atom (T_X), (ii) on the top of an nitrogen atom (T_N), and (iii) above the center of a hexagon ring (hollow (H) site) as illustrated in Figure 1 (a). As initial configurations, Li atom is placed 2 Å above the surface of h-XN plane in z-direction on considered sites. After optimization, we calculated the Li adsorption energy using following equation:

$$E_{\text{ads}} = \text{E(h} - \text{XN)} + \text{E(Li)} - E_{\text{tot}}\text{(Li@h} - \text{XN)} \quad (1)$$

where E_{ads} corresponds to the adsorption energy, E(h-XN) represents the total energy of bare h-XN monolayers, E(Li) is the free energy of an isolated single Li atom, E_{tot}(Li@h-XN) is the total energy of Li adsorbed h-XN system. $E_{\text{ads}} > 0$ represents the adsorption of the Li atom on the relevant site. Obtained adsorption energies for the each considered adsorption sites are demonstrated in Figure 2 (a). As is seen from Figure 2 (a), the H site is the most favorable adsorption site of Li atom for all considered h-XN structures. This favorable adsorption site is followed by T_X and T_N for both h-AlN and h-GaN while this order is vice versa in h-BN. We computed the adsorption energy of stably adsorbed Li atom at H site on h-BN as 0.279 eV. In a previous study, Hwang et al. [26] also found the H site as the most stable adsorption site of Li atom on h-BN monolayer with adsorption energy of 0.275 eV. We calculated the adsorption energies of a single Li atom at H, T_{Al} and T_N sites on h-AlN plane as 1.241, 0.938 and 0.885 eV (in respective order), which are close to the reported theoretical results in the literature. In this recent study, Sengupta [27] computed the adsorption energies as 1.510,

1.165 and 1.138 eV for H, T_{Al} and T_N sites, respectively, using Grimme's DFT-D2 method within QE and norm-conserving Troullier-Martins pseudopotential sets. We obtained the highest adsorption energy for H site on h-GaN plane with a value of 1.684 eV, as compared to h-BN and h-AlN. These adsorption energy values for the Li atom on h-XN are smaller than that obtained for germanene and stanene (2.07~2.21 eV) [14, 45-47].

We obtained electron charge density difference for a single Li atom adsorbed on the hollow site of each h-XN as in Figure 2 (b-d). The charge density differences (Δρ) obtained according to the following formula:

$$\Delta\rho = \rho_{\mathrm{Li@h-XN}} - \rho_{\mathrm{h-XN}} - \rho_{\mathrm{Li}} \tag{2}$$

where $\rho_{\mathrm{Li@h-XN}}$ means the charge density of monolayer after Li adsorption, $\rho_{\mathrm{h-XN}}$ represents the charge density of monolayer, and ρ_{Li} represents the charge density of Li.

As depicted in Figure 2 (b-d), electronic band structures of the h-XN monolayers have been significantly affected by Li adsorption. The energy levels of the valence and conduction bands shift to lower energy values due to charge transfer from Li adatom to the surface. Impurity band appears at the Fermi level of each h-XN electronic band structures and the all considered semiconducting h-XN monolayers start to exhibit metallic characteristic. The changes in the electronic structures, increase electrical conductivity of the systems and make them suitable materials as the anode of the Li-ion batteries. From projected DOS plots, it is obvious that the dominant orbital of the new energy band around the Fermi level comes from *s* orbital of the Li adatom.

To determine the diffusion barrier energy of a single Li atom diffusion along the surface between the two nearest neighbour hollow sites we performed the NEB calculations. Obtained energy barriers are illustrated in Figure 3. As can be seen from the Figure 2 (a), there are very small adsorption energy differences between the possible adsorption sites for the Li atom on h-BN monolayer, so there is only one global minimum for the diffusion path. The possible diffusion pathway of the Li atom on h-BN was obtained as H site to the bridge site over a BN bond and then H site. However, there is a local minimum while Li adatom diffuse on h-AlN or h-GaN monolayers. The diffusion path of Li in both h-AlN and h-GaN proceed to lie through H site-T_N-H site. The calculated migration barrier energies of Li ion on h-BN, h-AlN and h-GaN monolayers as approximately Δ= 0.117, 0.452, and 0.610 eV, respectively (Figure 3). The diffusion of Li on h-BN surface is much easier as compared to h-AlN and h-GaN monolayers and its value is comparable with a number of 2D materials such as MoO_2 (0.158 eV), MoS_2 (0.19-0.25 eV), WO_2 (0.176 eV), graphene (0.277 eV) and stanene (0.1-0.25 eV) [14,15,48-51]. However, the diffusion energy barriers of h-AlN and h-GaN monolayers are much better than that of phosphorene (0.76 eV) and silicene (1.2 eV) [11-14]. In the recent study of Sengupta [27], the diffusion energy barriers through the pathway of H-T_{Al}-H were reported as 0.40 eV and 0.45 eV for H-T_N-H pathway. In addition, we calculated the diffusion coefficient (D) using Arrhenius equation:

$$\mathrm{D} \cong a^2 \upsilon \exp\left(\frac{-\Delta}{k_B T}\right) \tag{3}$$

where a is the lattice constant of h-XN monolayer, D is the calculated Li diffusion energy barrier, $\upsilon = 10^{11}$ Hz, and k_BT = 0.026 eV [52,53]. The diffusion coefficient values were given in Table 1. Obtained diffusion coefficient values are comparable or higher than the commercially available Li-ion batteries [53,54]. However, we should note that increment of the diffusion energy barrier from the h-BN to the hAlN and h-GaN results in decreasing the diffusion coefficient value on the order of 10^{-5} and 10^{-8}, respectively. The low diffusion barrier energy and the high diffusion coefficient value of h-BN+Li system, indicates that the transport of the lithium ions on the h-BN monolayer along the considered diffusion path can be easily. However, the diffusion coefficients for Li ions along the two neighbour H sites on h-AlN and especially on h-GaN are small, which means poor possibility of Li ion mobility at the room temperature. But, as can be seen from the Equation 3, increasing of the temperature can increase the mobility of the Li ions on the substrates.

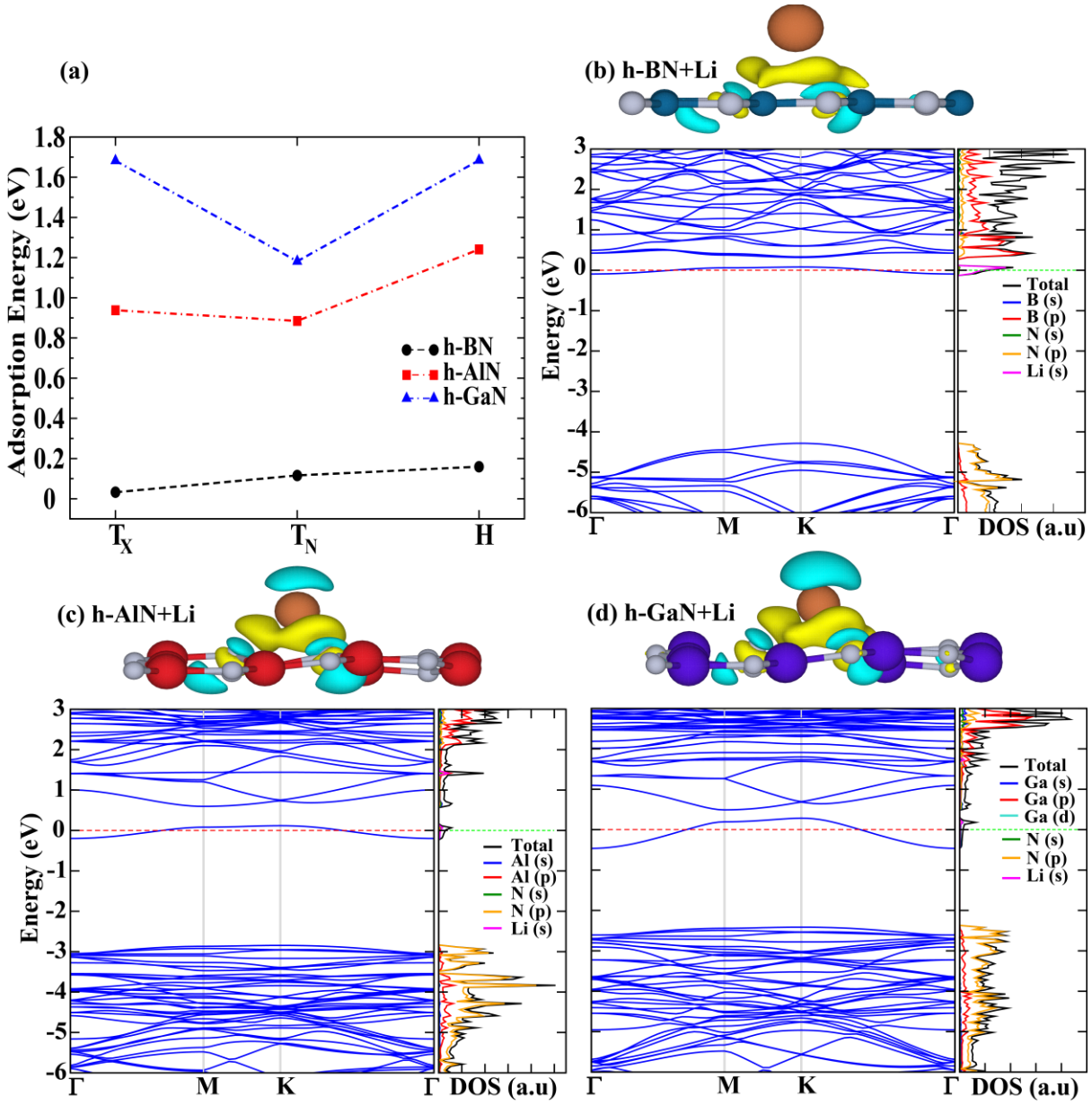


Figure 2. (a) Adsorption energies (eV) as a function of adsorption sites for h-XN (X=B, Al, Ga) monolayer structures. (b-d) On the above figures, isosurface plot of the charge density difference ($\Delta\rho$) for the adsorbed Li atom at the most stable site (H site) are illustrated. The isosurface level is set to 0.002 electrons/$Å^3$. The below figures are the electronic energy band structure, total and projected density of states (PDOS) for adsorbed single Li atom at H site of h-BN, h-AlN and h-GaN supercell structures.

Table 1. Calculated adsorption energy values for most favorable adsorption site (Hollow-site) of Li atom: Site, favorable adsorption site; h, the height of the stably adsorbed Li atom above h-

XN (X=B, Al, Ga) plane and D, the value of diffusion coefficient. A single Li atom has been placed 2 Å above the substrate atoms in z-direction.

Monolayer	E_{ads} (eV)	h (Å)	D(cm^2/s)
h-BN+Li	0.159	1.936	$7.00x10^{-7}$
h-AlN+Li	1.241	1.617	$2.73x10^{-12}$
h-GaN+Li	1.684	1.541	$6.66x10^{-15}$

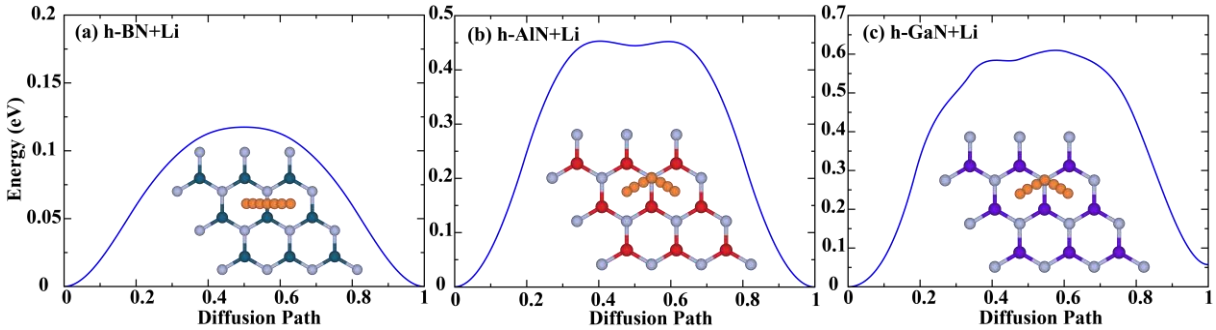


Figure 3. Calculated diffusion energy barriers of single Li atom adsorbed on h-XN (X=B, Al, Ga) monolayer structures along a diffusion path.

4. CONCLUSION

Using first principle calculations with the Grimme's DFT-D2 dispersion correction, we explore the favorable adsorption site of the Li adatom on the h-BN, h-AlN and h-GaN monolayer structures upon three different adsorption sites. We obtained that the hollow site is the most preferable adsorption site of a single Li atom on h-XN monolayer. The hollow site of h-GaN offers the highest adsorption energy for Li atom in comparison to h-BN and h-AlN. We also determined the lithium diffusion barrier energy for these monolayer structures. Our results show, calculated barrier energy on h-BN is lower than the most of 2D monolayers, while diffusion energies for h-AlN and h-GaN are lower or comparable with the commercial Li-ion batteries. Li adsorption leads to a change in electronic band structure of each considered monolayers and semiconductor characteristic with wide band gap is turned into metallic, which is preferable electronic structure property for the anode electrodes. Our results show that the h-XN monolayers would be promising candidate anode materials for Li-ion batteries, due to their adsorption energies and suitable diffusion energy barriers. Also, their metallic character after Li adsorption makes them good conductor and preferable materials.

ACKNOWLEDGEMENTS

Computing resources used in this work were provided by the TUBITAK ULAKBIM, High Performance and Grid Computing Center (Tr-Grid e-Infrastructure).

REFERENCES

[1] Armand M, Tarascon JM. Building better batteries. Nature 2008; 451(7179): 652.

[2] Croguennec L, Palacin MR. Recent achievements on inorganic electrode materials for lithium-ion batteries. J Am Chem Soc. 2015; 137(9):3140-56.

[3] Prosini PP, Cento C, Carewska M, Masci A. Electrochemical performance of Li-ion batteries assembled with water-processable electrodes. Solid State Ionics. 2015; 274:34-9.

[4] Kino K, Yonemura M, Ishikawa Y, Kamiyama T. Two-dimensional imaging of charge/discharge by Bragg edge analysis of electrode materials for pulsed neutron-beam transmission spectra of a Li-ion battery. Solid State Ionics. 2016; 288:257-61.

[5] Johannes MD, Swider-Lyons K, Love CT. Oxygen character in the density of states as an indicator of the stability of Li-ion battery cathode materials. Solid State Ionics. 2016 Mar 31;286:83-9.

[6] Li H, Wang Z, Chen L, Huang X. Research on advanced materials for Li‐ion batteries. Adv Mater. 2009; 21(45):4593-607.

[7] Shi S, Gao J, Liu Y, Zhao Y, Wu Q, Ju W, Ouyang C, Xiao R. Multi-scale computation methods: Their applications in lithium-ion battery research and development. Chinese Phys B. 2015; 25(1):018212.

[8] Etacheri V, Marom R, Elazari R, Salitra G, Aurbach D. Challenges in the development of advanced Li-ion batteries: a review. Energ Environ Sci. 2011; 4(9):3243-62.

[9] Wang G, Shen X, Yao J, Park J. Graphene nanosheets for enhanced lithium storage in lithium ion batteries. Carbon. 2009 Jul 1;47(8):2049-53.

[10] Fan X, Zheng WT, Kuo JL, Singh DJ. Adsorption of single Li and the formation of small Li clusters on graphene for the anode of lithium-ion batteries. ACS Appl Mater Inter. 2013; 5(16): 7793-7.

[11] Zhao S, Kang W, Xue J. The potential application of phosphorene as an anode material in Li-ion batteries. J Mater Chem A. 2014; 2(44): 19046-52.

[12] Jiang HR, Lu Z, Wu MC, Ciucci F, Zhao TS. Borophene: a promising anode material offering high specific capacity and high rate capability for lithium-ion batteries. Nano Energy. 2016; 23:97-104.

[13] Zhang Y, Wu ZF, Gao PF, Zhang SL, Wen YH. Could Borophene be used as a promising anode material for high-performance lithium ion battery?. ACS Appl Mater Inter. 2016; 8(34): 22175-81.

[14] Mortazavi B, Dianat A, Cuniberti G, Rabczuk T. Application of silicene, germanene and stanene for Na or Li ion storage: A theoretical investigation. Electrochim Acta. 2016; 213:865-70.

[15] Sengupta A, Frauenheim T. Lithium and sodium adsorption properties of monolayer antimonene. Mater Today Energy. 2017; 5:347-54.

[16] Zhang X, Liu Z, Hark S. Synthesis and optical characterization of single-crystalline AlN nanosheets. Solid State Commun. 2007; 143(6-7):317-20.

[17] Golberg D, Bando Y, Huang Y, Terao T, Mitome M, Tang C, Zhi C. Boron nitride nanotubes and nanosheets. ACS Nano. 2010; 4(6):2979-93.

[18] Tsipas P, Kassavetis S, Tsoutsou D, Xenogiannopoulou E, Golias EG, Giamini SA, Grazianetti C, Chiappe D, Molle A, Fanciulli M, Dimoulas A. Evidence for graphite-like hexagonal AlN nanosheets epitaxially grown on single crystal Ag (111). Appl Phys Lett. 2013; 103(25): 251605.

[19] Samadizadeh M, Rastegar SF, Peyghan AA. F−, Cl−, Li+ and Na+ adsorption on AlN nanotube surface: a DFT study. Physica E. 2015; 69:75-80.

[20] Zeng H, Zhi C, Zhang Z, Wei X, Wang X, Guo W, Bando Y, Golberg D. "White graphenes": boron nitride nanoribbons via boron nitride nanotube unwrapping. Nano Lett. 2010; 10(12): 5049-55.

[21] Ma D, Lu Z, Ju W, Tang Y. First-principles studies of BN sheets with absorbed transition metal single atoms or dimers: stabilities, electronic structures, and magnetic properties. J Phys-Condens Mat. 2012; 24(14): 145501.

[22] Zhou YG, Xiao-Dong J, Wang ZG, Xiao HY, Gao F, Zu XT. Electronic and magnetic properties of metal-doped BN sheet: A first-principles study. Phys Chem Chem Phys. 2010; 12(27): 7588-92.

[23] Zhou YG, Zu XT, Yang P, Xiao HY, Gao F. Oxygen-induced magnetic properties and metallic behavior of a BN sheet. J Phys-Condens Mat. 2010; 22(46): 465303.

[24] Li J, Hu ML, Yu Z, Zhong JX, Sun LZ. Structural, electronic and magnetic properties of single transition-metal adsorbed BN sheet: A density functional study. Chem Phys Lett. 2012; 532:40-6.

[25] Anaraki-Ardakani H. A computational study on the application of AlN nanotubes in Li-ion batteries. Phys Lett A. 2017; 381(11):1041-6.

[26] Hwang Y, Chung YC. Lithium adsorption on hexagonal boron nitride nanosheet using dispersion-corrected density functional theory calculations. Jpn J Appl Phys. 2013; 52(6S): 06GG08.

[27] Sengupta A. Lithium and sodium adsorption properties of two-dimensional aluminum nitride. Appl Surf Sci. 2018; 451:141-7.

[28] Giannozzi P, Baroni S, Bonini N, Calandra M, Car R, Cavazzoni C, Ceresoli D, Chiarotti GL, Cococcioni M, Dabo I, Dal Corso A. QUANTUM ESPRESSO: a modular and open-source software project for quantum simulations of materials. J Phys-Condens Mat. 2009; 21(39): 395502.

[29] Perdew JP, Burke K, Ernzerhof M. Generalized gradient approximation made simple. Phys Rev Lett. 1996; 77(18): 3865.

[30] Kresse G, Joubert D. From ultrasoft pseudopotentials to the projector augmented-wave method. Phys Rev B. 1999; 59(3): 1758.

[31] Grimme S. Semiempirical GGA-type density functional constructed with a long-range dispersion correction. J Comput Chem. 2006; 27(15): 1787-99.

[32] Monkhorst HJ, Pack JD. Special points for Brillouin-zone integrations. Phys Rev B. 1976; 13(12): 5188.

[33] Head JD, Zerner MC. A Broyden—Fletcher—Goldfarb—Shanno optimization procedure for molecular geometries. Chem Phys Lett. 1985; 122(3): 264-70.

[34] Davidson ER. The iterative calculation of a few of the lowest eigenvalues and corresponding eigenvectors of large real-symmetric matrices. J Comput Phys. 1975; 17:87-94.

[35] Henkelman G, Uberuaga BP, Jónsson H. A climbing image nudged elastic band method for finding saddle points and minimum energy paths. J Chem Phys. 2000; 113(22): 9901-4.

[36] Zhang CW. First-principles study on electronic structures and magnetic properties of AlN nanosheets and nanoribbons. J Appl Phys. 2012; 111(4):043702.

[37] Rastegar SF, Peyghan AA, Ghenaatian HR, Hadipour NL. NO2 detection by nanosized AlN sheet in the presence of NH3: DFT studies. Appl Surf Sci. 2013; 274:217-20.

[38] Ahmadi Peyghan A, Soleymanabadi H, Bagheri Z. Hydrogen release from NH3 in the presence of BN graphene: DFT studies. J Mex Chem Soc. 2015; 59(1): 67-73.

[39] Hosseinian A, Khosroshahi ES, Nejati K, Edjlali E, Vessally E. A DFT study on graphene, SiC, BN, and AlN nanosheets as anodes in Na-ion batteries. J Mol Model. 2017; 23(12): 354.

[40] Kecik D, Onen A, Konuk M, Gürbüz E, Ersan F, Cahangirov S, Aktürk E, Durgun E, Ciraci S. Fundamentals, progress, and future directions of nitride-based semiconductors and their composites in two-dimensional limit: A first-principles perspective to recent synthesis. Appl Phys Rev. 2018; 5(1): 011105.

[41] Wilkinson G, Stone FG, Abel EW. Comprehensive organometallic chemistry. Pergamon Press; 1982.

[42] Huheey JE, Keiter EA, Keiter RL, Medhi OK. Inorganic chemistry: principles of structure and reactivity. Pearson Education India; 2006.

[43] Ersan F, Gökoğlu G, Aktürk E. Bimetallic two-dimensional PtAg coverage on h-BN substrate: First-principles calculations. Appl Surf Sci. 2014; 303: 306-11.

[44] Ersan F. Platinum Adsorption and Diffusion on Two-Dimensional Gallium Nitride. Süleyman Demirel University J Natural and Appl Sci 2018; 22 (2): 393-396.

[45] Tritsaris GA, Kaxiras E, Meng S, Wang E. Adsorption and diffusion of lithium on layered silicon for Li-ion storage. Nano Lett. 2013; 13(5):2258-63.

[46] Lin X, Ni J. Much stronger binding of metal adatoms to silicene than to graphene: a first-principles study. Phys Rev B. 2012; 86(7):075440.

[47] Osborn TH, Farajian AA. Stability of lithiated silicene from first principles. J Phys Chem C. 2012;116(43):22916-20.

[48] Chen HJ, Huang J, Lei XL, Wu MS, Liu G, Ouyang CY, Xu B. Adsorption and diffusion of lithium on MoS_2 monolayer: the role of strain and concentration. Int J Electrochem Sci. 2013;8(2):2196-203.

[49] Stephenson T, Li Z, Olsen B, Mitlin D. Lithium ion battery applications of molybdenum disulfide (MoS_2) nanocomposites. Energ Environ Sci. 2014;7(1):209-31.

[50] Ersan F, Ozaydin HD, Gökoğlu G, Aktürk E. Theoretical investigation of lithium adsorption, diffusion and coverage on MX2 (M= Mo, W; X= O, S, Se, Te) monolayers. Appl Surf Sci. 2017; 425:301-6.

[51] Zhou LJ, Hou ZF, Wu LM. First-principles study of lithium adsorption and diffusion on graphene with point defects. J Phys Chem C. 2012; 116(41):21780-7.

[52] Van der Ven A, Ceder G. First principles calculation of the interdiffusion coefficient in binary alloys. Phys Rev Lett. 2005; 94(4):045901.

[53] Wang H, Wang X, Wang L, Wang J, Jiang D, Li G, Zhang Y, Zhong H, Jiang Y. Phase transition mechanism and electrochemical properties of nanocrystalline MoSe2 as anode materials for the high performance lithium-ion battery. J Phys Chem C. 2015; 119(19): 10197-205.

[54] Yu P, Popov BN, Ritter JA, White RE. Determination of the lithium ion diffusion coefficient in graphite. J Electrochem Soc. 1999; 146(1):8-14.